Micromachines **2014**, *5*, 859-867; doi:10.3390/mi5040859

OPEN ACCESS

micromachines

ISSN 2072-666X

www.mdpi.com/journal/micromachines

Article

Simulation Study on Polarization-Independent Microlens Arrays Utilizing Blue Phase Liquid Crystals with Spatially-Distributed Kerr Constants

Hung-Shan Chen, Michael Chen, Chia-Ming Chang, Yu-Jen Wang and Yi-Hsin Lin *

Department of Photonics, National Chiao Tung University, Hsinchu 30010, Taiwan;
E-Mails: convince.eo98g@g2.nctu.edu.tw (H.-S.C.); michaelchen.eo01g@g2.nctu.edu.tw (M.C.); spp02042003.eo02g@nctu.edu.tw (C.-M.C.); wangyujen.eo02g@g2.nctu.edu.tw (Y.-J.W.)

* Author to whom correspondence should be addressed; E-Mail: yilin@mail.nctu.edu.tw (Y.-H.L.); Tel.: +886-3571-2121 (ext. 56376).

External Editor: Hongrui Jiang

Received: 23 June 2014; in revised form: 3 September 2014 / Accepted: 28 September 2014 / Published: 3 October 2014

Abstract: Polarization independent liquid crystal (LC) microlens arrays based on controlling the spatial distribution of the Kerr constants of blue phase LC are simulated. Each sub-lens with a parabolic distribution of Kerr constants results in a parabolic phase profile when a homogeneous electric field is applied. We evaluate the phase distribution under different applied voltages, and the focusing properties of the microlens arrays are simulated. We also calculate polarization dependency of the microlenses arrays at oblique incidence of light. The impact of this study is to provide polarizer-free, electrically tunable focusing microlens arrays with simple electrode design based on the Kerr effect.

Keywords: Kerr effect; microlenses; polarization independent; liquid crystal; blue phase

---

1. Introduction

Liquid crystal (LC) microlens arrays are important in applications of 2D/3D switching, fiber coupling, and sensors [1–3]. Most of proposed structures of LC microlens arrays require at least one polarizer. To remove the usage of a polarizer, polarization independent LC phase modulations are developed. Three types of polarization independent LC phase modulations have been proposed: the type of the double-layered structure, the type of the residual phase structure, and the mixed type [4–10].

However, the structures were relatively complicated and the response times were slow. In 2010, we proposed a polarization independent polymer stabilized blue phase liquid crystal (PSBP-LC) microlens arrays based on the electric-field-induced Kerr effect, the field-induced birefringence is proportional to the electric field squared [11]. The Kerr effect exists in many LC materials, such as polymer stabilized isotropic phase liquid crystals, nematic liquid crystals, blue phase liquid crystals, and even ferroelectric liquid crystals [12–14]. In this paper, we proposed polarization independent LC microlens arrays based on controlling the distribution of the Kerr constants of blue phase LC (BPLC). The simulated results indicate the distribution of the Kerr constants of BPLC results in a parabolic optical phase shift and the proposed microlens arrays are capable of imaging. The polarization dependency of the LC microlens arrays is also discussed. The purpose of this study is mainly to provide a way to achieve polarizer-free, electrically tunable focusing microlens arrays with simple electrode design based on the Kerr effect.

2. Operating Principle and Lens Design

The Kerr medium, such as BPLC and PSBP-LC, is optically isotropic without an external electric field [11]. Under an external electric field (E), the optical axis of the field-induced birefringence is parallel to the electric field. The field-induced birefringence (Δn) is written as [15]:

$$\Delta n = n_e(E) - n_o(E) = \lambda \cdot K \cdot E^2 \tag{1}$$

where n_o is ordinary refractive index, n_e is extraordinary refractive index, K is the Kerr constant of the LC materials, and λ is wavelength of the incident light. Regarding the local orientations of LC molecules of BPLC under external electric field, $n_o(E)$ and $n_e(E)$ can be further expressed in Equations (2) and (3):

$$n_o(E) = n_{ave} - \frac{\lambda \cdot K \cdot E^2}{3} \tag{2}$$

$$n_e(E) = n_{ave} + \frac{2}{3} \cdot \lambda \cdot K \cdot E^2 \tag{3}$$

where n_{ave} represents the average refractive index without any applied electric field (*i.e.*, $n_{ave} = (n_e + 2n_o)/3$). As a result, polarization independent phase modulation based on the Kerr effect of LC materials can be achieved. To generate a corresponding polarization independent phase profile of a lens, an inhomogeneous electric field is a way to be adopted [11]. However, the patterned electrodes are required. Instead of patterned electrodes, we proposed a spatially-distributed Kerr constant to achieve polarization independent microlens arrays. The structure and operating principles are depicted in Figure 1a,b. The structure primary consists of LC materials and two glass substrates coated with a layer of indium-tin-oxide (ITO). Without an applied voltage (V), an incident unpolarized light propagating along z-direction sees the average refractive index of n_{ave} because the effective optical index-ellipsoids are spherical which means the LC material is optically isotropic due to the cubic symmetry of the lattice structure, as depicted in Figure 1a [11,16]. With an applied voltage, an incident unpolarized light sees a spatial optical phase difference originating from a spatial distribution of Kerr constants, as depicted in Figure 1b. Assume the Kerr constant is spatially distributed in a parabolic form which can be expressed as:

$$K(r) = K_c - \frac{K_c - K_b}{r_0^2} \cdot r^2 \tag{4}$$

where r_0 is the radius of aperture of a sub-lens, r is position, K_c is the Kerr constant at the center of the aperture, and K_b is the Kerr constant around the peripheral region. Optical phase difference (OPD) under an applied voltage ($\delta(r)$) is $2\pi/\lambda \cdot [n_o(E) \cdot d]$, where d is the cell gap. From Equations (2) and (4), OPD is:

$$\delta(r) = \frac{2\pi}{\lambda} \times d \times \left[n_{ave} - \frac{\lambda \times E^2}{3} \times \left(K_c - \frac{K_c - K_b}{r_0^2} r^2 \right) \right] \tag{5}$$

r^2 term in Equation (4) is related to the focal length (f), inverse of lens power (P) [17,18]. Lens power is the degree that a lens converges or diverges light. The unit of lens power is diopter (D or m^{-1}). Thereafter, the lens power is written as:

$$P(E) = -\frac{2 \times \lambda \times d \times E^2 \times (K_c - K_b)}{3 \times r_0^2} = -\frac{2 \times \lambda \times d \times E^2 \times \Delta K}{3 \times r_0^2} \tag{6}$$

where ΔK is defined as $(K_c - K_b)$. Thus, we can realize microlens arrays based on spatially- distributed Kerr constants whose lens power is electrically tunable. The lens power of the mocrolens arrays is larger as both the applied electric field and ΔK are larger.

Figure 1. The structure and operating principles of the LC (liquid crystal) microlens arrays (**a**) without an applied voltage and (**b**) with an applied voltage.

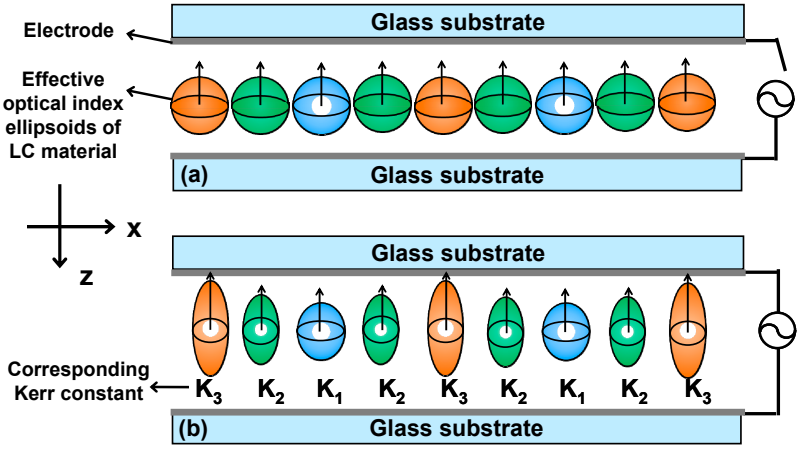

3. Simulation Results and Discussion

Here we simulate LC microlens arrays with spatially-distributed Kerr constants. The designed aperture size and the spacing between adjacent sub-lenses are 100 μm. The cell gap of the LC lenses is 25 μm. Usually Kerr constant is in a range between 10^{-8} and 10^{-10} V^2/m [19–21]. To demonstrate microlens arrays with a positive focal length, we design the Kerr constant in the center of a sub-lens (K_c) is 10^{-8} V^2/m while the Kerr constant at the peripheral region of a sub-lens (K_b) is 10^{-9} V^2/m. Figure 2 plots the parabolic distribution of Kerr constants of the microlens arrays based on the parameters we designed. We defined the phase shift as the difference between OPD at an applied voltage (V) and at $V = 0$. From Figure 2a and Equation (5), the phase shift as a function of position is shown in Figure 2b. The curve of phase shift in Figure 2b exhibits a periodically parabolic form at $V > 0$

due to the parabolic distribution of Kerr constant of the LC layer. The phase shift increases with an applied voltage. Based on Equation (6) and the parabolic distribution we designed, the simulated voltage-dependent lens power is depicted in Figure 2c. The lens power increases with an applied voltage. The lens power at V = 100 V_{rms} is around 650 m^{-1}, which is corresponding to the focal length of ~1.54 mm.

Figure 2. (**a**) The spatial distribution of Kerr constants of the LC microlens arrays based on the parameters we designed; (**b**) the corresponding spatial phase shift of the LC microlens arrays at V = 0 (red line), 50 V_{rms} (green line), and 100 V_{rms} (blue line); and (**c**) the simulated voltage- dependent lens power.

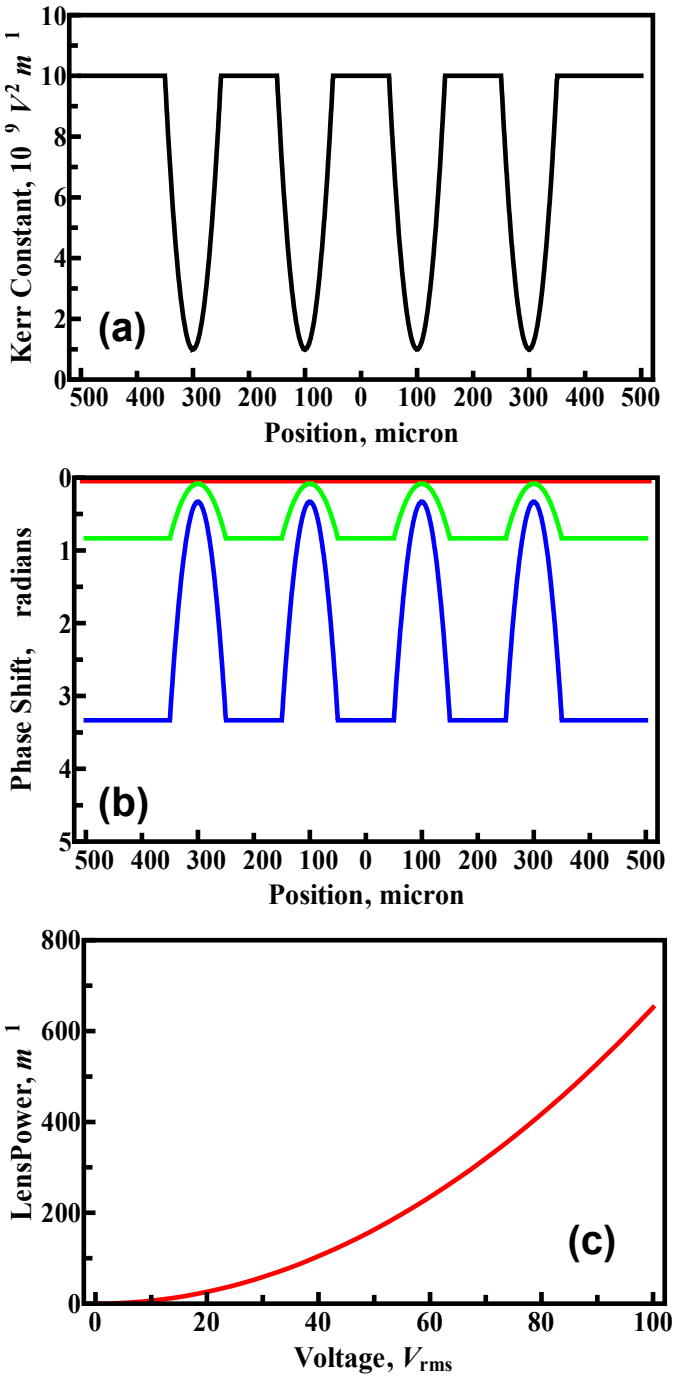

To simulate the focusing properties of the microlens arrays at the focal plane, we adopted the Fresnel approximation [22]. Figure 3a,b shows the spatial phase shift and corresponding intensity distribution at the focal plane of the micolens arrays. As we can see, the parabolic phase shift (red line in Figure 3a results in sharp peaks at the focal plane (red line in Figure 3b). In contrast, the trapezoid-like phase shift (blue dotted line in Figure 3a) results in relatively broad peaks at the focal plane (blue dotted line in Figure 3b). Therefore, the parabolic phase distribution is necessary to realize good imaging quality which also means the distribution of Kerr constants should be parabolic. In 2011, Wu *et al.* proposed an Eiffel-Tower-like ITO electrode to generate an ideal phase distribution in BPLC [23]. However, the Eiffel-Tower-like ITO electrode is difficult to fabricate. The method of the spatial distribution of Kerr constants that we proposed is more practical because our method does not require complex electrodes.

Figure 3. (**a**) The simulated spatial phase shifts of the LC microlens arrays. Blue dotted line stands for periodically trapezoid-like phase shift and red line stands for periodically parabolic phase shift; (**b**) the corresponding intensity distribution at the focal plane for the periodically trapezoid-like phase shift (dotted blue line) and the periodically parabolic phase shift (red line).

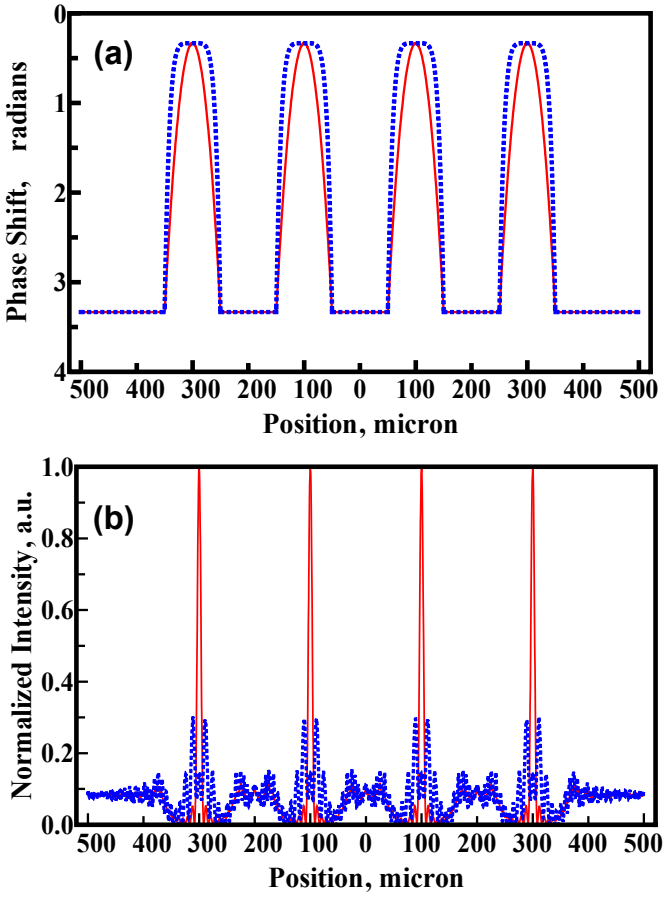

The LC microlens arrays as incident light is at the oblique angle (*i.e.*, off-axis) is also important in applications. Assume the incident angle is θ_i with respect to *z*-direction and the light propagates in LC cell with an angle of θ_{LC}. Because the change of the refractive index of the Kerr medium is very small (normally < 0.05), we can assume the incident light propagates in a straight way in the medium and θ_{LC}

is able to be deduced from Snell's law (*i.e.*, $n_{air} \times \sin\theta_i = n_{ave} \times \sin\theta_{LC}$). Two eigenmodes propagating in the LC medium are defined as e-mode and the o-mode. The polarization of e-mode lies in the plane of *x*-*z* plane and that of o-mode is perpendicular to *x*-*z* plane. Thereafter, we can calculate the phase shift of the e-mode as:

$$\delta_{e-mode}(E,x) = \frac{2\pi}{\lambda}\int n_{e,eff}(E,\theta_{LC},x)\cdot dk = \frac{2\pi}{\lambda}\int n_{e,eff}(E,\theta_{LC},x)\cdot \csc\theta_{LC}\cdot dx \quad (7)$$

where the effective extraordinary refractive index ($n_{e,eff}$) can be expressed as:

$$n_{e,eff}(E,\theta_{LC},x) = \left(\frac{n_e^2(E,x)}{\sin^2(\theta_{LC})} + \frac{n_o^2(E,x)}{\cos^2(\theta_{LC})}\right)^{-0.5} \quad (8)$$

The phase shift of the o-mode can also be expressed as:

$$\delta_{o\text{-}mode}(E,x) = \frac{2\pi}{\lambda}\int n_o(E,x)\cdot dk = \frac{2\pi}{\lambda}\int n_o(E,x)\cdot \csc\theta_{LC}\cdot dx \quad (9)$$

To simplify the discussion, a single sub-lens is considered in the following discussions. The diameter of the sub-lens and the cell gap are 100 and 25 μm, respectively. The simulated phase shifts as incident light is at the oblique angle are shown in Figure 4. The dotted line represents the phase shift of e-mode while the solid line represents the o-mode at V = 100 V_{rms}. The blue and the red represent θ_{LC} of ~+10° and −10°, respectively. From Snell's law, θ_i is ~±15.7° when corresponding θ_{LC} is ±10° and n_{ave} is around 1.56. From the simulation results, the phase shift between the center and the peripheral region for the e-mode is around 3π radians. As to the o-mode, the phase shift between the center and the peripheral region is around ~2.8π. This also indicates the micorlens arrays are polarization dependent at the oblique incidence because the refractive index changes more for o-ray than that for e-ray. To reduce the polarization dependency of the phase shift at oblique incidence, we can use other electrically tunable LC cells for phase compensation.

To experimentally realize the spatial distribution of the Kerr constants of the LC materials, one can produce the spatial distribution of Kerr constants of the Kerr medium, such as BPLC, in terms of fabrication method of spatial temperature gradient. Based on previous research results, the Kerr constant is proportional to the coherent length squared (ξ^2), inversely proportional to $T-T^*$, where T is temperature and T^* represents the temperature as the coherent length of the LC become infinite (*i.e.*, $K \propto \xi^2 \propto 1/T-T^*$) [19–21]. As a result, the Kerr constant of BPLC strongly depends on the temperature. Therefore, the spatial distribution of the Kerr constant can be controlled by means of temperature gradient, and then we can use photo-polymerization to stabilize BPLC in order to regulate the distribution of phase separation and further to generate spatially-distributed Kerr constants. To demonstrate the proposed idea, we step-controlled the curing temperatures of the PSBP-LC materials, and we realized the Kerr constant difference check by phase retardation measurement three times. However, due to the limit of the temperature gradient controlling instrument, we are not able to put such a big Kerr constant difference within this small aperture region. For further implementation of this concept, one might need step masks or more precision thermal controlling machines to get steep phase distribution within the aperture.

Figure 4. The simulated phase shift at the oblique angle. The dotted line represents the phase shift of o-mode and the solid line represents the phase shift of e-mode. The blue and red represent the incident angle θ_i is +15.7° and −15.7°, respectively.

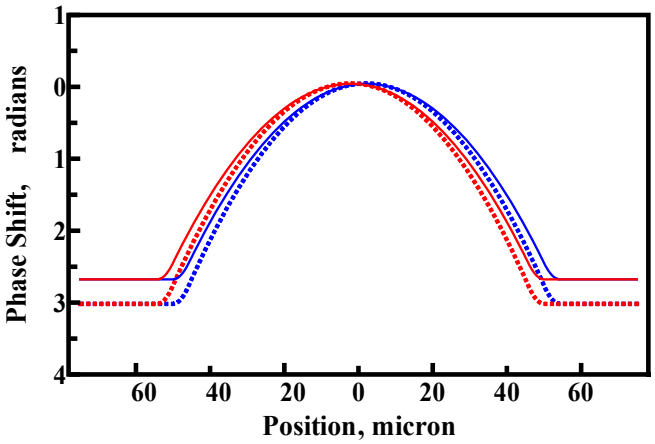

4. Conclusions

We proposed a polarization independent LC microlens arrays based on spatially distributed Kerr constants of the LC material. The mechanism and simulated performance are discussed. In addition, we also evaluate the polarization dependency of the microlens arrays at oblique angle of incidence. This study provides a method to realize polarizer-free and electrically tunable microlens arrays with simple electrodes based on the Kerr effect.

Acknowledgments

This research was supported partially by the Ministry of Science and Technology (MOST) in Taiwan under the contract No. NSC 101-2112-M-009-011-MY3.

Author Contributions

Hung-Shan Chen proposed the concept, did the simulation and wrote the manuscript. Michael Chen, Chia-Ming Chang, and Yu-Jen Wang helped in the simulations and discussions. Yi-Hsin Lin discussed the concept and results with Hung-Shan Chen, and also revised the manuscript.

Conflicts of Interest

The authors declare no conflict of interest

References

1. Liu, Y.F.; Ren, H.W.; Xu, S.; Li, Y.; Wu, S.T. Fast-response liquid crystal lens for 3D displays. *SPIE Proc.* **2014**, *9005*, 1–10.
2. Chen, M.; Chen, C.H.; Lai, Y.; Lu, Y.C.; Lin, Y.H. An electrically tunable polarizer for a fiber system based on a polarization-dependent beam size derived from a liquid crystal lens. *IEEE Photonics J.* **2014**, *6*, 1–8.

3. Klaus, W.; Ide, M.; Hayano, Y.; Morokawa, S.; Arimoto, Y. Adaptive LC lens array and its application. *SPIE Proc.* **1999**, *3635*, 66–73.
4. Lin, Y.H.; Ren, H.W.; Wu, Y.H.; Zhao, Y.; Fang, J.Y.; Ge, B.Z.; Wu, S.H. Polarization-independent liquid crystal phase modulator using a thin polymer-separated double-layered structure. *Opt. Express* **2005**, *13*, 8746–8752.
5. Lin, Y.H.; Ren, H.W.; Fan, Y.H.; Wu, Y.H.; Wu, S.T. Polarization-independent and fast-response phase modulation using a normal-mode polymer-stabilized cholesteric texture. *J. Appl. Phys. Lett.* **2005**, *98*, doi:10.1063/1.2037191.
6. Ren, H.W.; Lin, Y.H.; Fan, Y.H.; Wu, S.T. Polarization-independent phase modulation using a polymer-dispersed liquid crystal. *Appl. Phys. Lett.* **2005**, *86*, doi:10.1063/1.1899749.
7. Wu, Y.H.; Lin, Y.H.; Lu, Y.Q.; Ren, H.; Fan, Y.H.; Wu, J.R.; Wu, S.T. Submillisecond response variable optical attenuator based on sheared polymer network liquid crystal. *Opt. Express* **2004**, *12*, 6382–6389.
8. West, J.L.; Zhang, G.Q.; Reznikov, Y.; Glushchenko, A. Fast birefringent mode of stressed liquid crystal. *Appl. Phys. Lett.* **2005**, *86*, doi:10.1063/1.1852720.
9. Ren, H.; Lin, Y.H.; Wen, C.H.; Wu S.T. Polarization-independent phase modulation of a homeotropic liquid crystal gel. *Appl. Phys. Lett*. **2005**, *87*, doi:10.1063/1.2126107.
10. Lin, T.H.; Chen, M.S.; Lin, W.C.; Tsou, Y.S. A polarization-independent liquid crystal phase modulation using polymer-network liquid crystals in a 90° twisted cell. *J. Appl. Phys. Lett.* **2012**, *112*, doi:10.1063/1.4737260.
11. Lin, Y.H.; Chen, H.S.; Lin, H.C.; Tsou, Y.S.; Hsu, H.K.; Li, W.Y. Polarizer-free and fast response microlens arrays using polymer-stabilized blue phase liquid crystals. *Appl. Phys. Lett.* **2010**, *96*, doi:10.1063/1.3360860.
12. Yang, Y.C.; Yang, D.K. Electro-optic Kerr effect in polymer-stabilized isotropic liquid crystals. *Appl. Phys. Lett.* **2011**, *98*, doi:10.1063/1.3533396.
13. Khoshsima, H.; Tajalli, H.; Ghanadzadeh Gilani, A.; Dabrowski, R. Electro-optical Kerr effect of two high birefringence nematic liquid crystals. *Appl. Phys. Lett.* **2006**, *39*, 1495–1499.
14. Pozhidaev, E.P.; Kiselev, A.D.; Srivastave, A.K.; Chigrinov, V.G.; Kwok, H.S.; Minchenko, M.V. Orientational "Kerr effect" and phase modulaion of light in deformed-helix ferroelectric liquid crystals with subwavelength pitch. *Phys. Rev.* **2013**, *87*, doi:10.1103/PhysRevE.87.052502.
15. Lin, Y.H.; Chen, H.S.; Wu, C.H.; Hsu, H.K. Measuring electric-field-induced birefringence in polymer stabilized blue phase liquid crystal based on phase shift measurement. *J. Appl. Phys.* **2011**, *109*, doi:10.1063/1.3583572.
16. Amnon, Y.; Yeh, P. *Optical Waves in Crystals: Propagation and Control of Laser Radiation*; Wiley: New York, NY, USA, 1984; p. 83.
17. Lin, H.C.; Chen, M.S.; Lin, Y.H. A review of electrically tunable focusing liquid crystal lenses. *Trans. Electr. Electron. Mater.* **2011**, *12*, 234–240.
18. Lin, Y.H.; Chen, H.S. Electrically tunable-focusing and polarizer-free liquid crystal lenses for ophthalmic applications. *Opt. Express* **2013**, *21*, 9428–9436.
19. Haseba, Y.; Kikuchi, H.; Nagamura, T.; Kajiyama, T. Large electr-optic Kerr effect in nanostructures chiral liquid-crystal composites over a wide temperature range. *Adv. Mater.* **2005**, *17*, 2311–2315.

20. Tian, L.; Goodby, J.W.; Gortz, V.; Gleeson, H.F. The magnitude and tmeperature dependence of the Kerr constant in liquid crystal blue phases and the dark conglomerate phase. *Liq. Crys.* **2013**, *40*, 1446–1454.
21. Majles Ara, M.H.; Mousavi, S.H.; Rafiee, M.; Zakerhamidi, M.S. Dtermination of temperature dependence of Kerr constant for nematic liquid crystal. *Mol. Cryst. Liq. Cryst.* **2011**, *544*, 227/[1215]–231/[1219]
22. Goodman, J.W. *Introduction to Fourier Optics*, 3rd ed.; Roberts and Company Publishers: Greenwood Village, CO, USA, 2005; p. 67.
23. Li, Y.; Wu, S.T. Polarization independent adaptive microlens with a blue-phase liquid crystal. *Opt. Express* **2011**, *19*, 8045–8050.